Calculations of the motion of non-uniform shock waves

By JAN ROŚCISZEWSKI
Pierce Hall, Harvard University

(Received 31 March 1959 and in revised form 30 January 1960)

Problems of the propagation of shock waves and strong detonation waves through ducts of variable cross-section and ducts with porous walls, and the interaction of a rarefaction wave with a shock and a contact surface in one-dimensional unsteady, or two-dimensional steady, flow are solved using a simple rule. Tables enclosed in this paper permit efficient calculation of several problems of non-uniform shock motion.

1. Introduction

The aim of this paper is to give a simple method of analysing various situations involving the motion of non-uniform shock waves. The method is a modified form of the characteristic rule given by Whitham (1958), or the methods given by Chisnell (1957) and the author (1958). The rule developed in this paper enables one to treat many cases of the motion of non-uniform shock waves with different boundary conditions. Whitham's characteristic rule is a special case of this method when a particular kind of boundary condition obtains.

The problems treated represent boundary-value problems for a system of partial differential equations, in which one boundary condition is given on one line, and on another unknown line (the shock locus) a second boundary condition is defined by compatibility equations. The rule of this paper enables the behaviour of the shock wave to be calculated without solving the system of partial differential equations governing the flow.

Some of the problems discussed below have been solved by the use of methods differing from the present one. Some very practicable step-by-step methods for difference equations are discussed by Courant & Friedrichs (1948). The problem of the propagation of shock waves through a duct of variable cross-section was solved by Chisnell (1957), for the case when the gas in front of the shock is at rest. Another method of solving this problem was given by the author (1958). In the present paper, shock-wave propagation through ducts of variable cross-section, when a given non-uniform steady flow exists ahead of the shock wave, is discussed.

The interaction of a simple wave and a shock wave was solved in a closed form by Friedrichs (1948) for the case of weak shocks where the entropy changes may be neglected. The influence, of a slow perturbation of the otherwise uniform piston motion on a shock wave, was discussed by Gundersen (1958). The present

method gives good results for arbitrary shock strength and arbitrary piston motion.

A similar procedure applied to the case of plane hypersonic flow around a profile gives better results than the shock expansion method.*

2. General relations for unsteady non-isentropic flow in ducts

The system of equations governing unsteady non-isentropic flow behind a shock wave in a duct can be written in the characteristic form

$$\frac{\partial r}{\partial \alpha} \equiv \frac{\partial r}{\partial t} + (V+a)\frac{\partial r}{\partial x} = \frac{a}{2c_p(k-1)}\frac{\partial S}{\partial \alpha} - \frac{a}{2}\frac{D\ln A}{Dt} + F(a, V, x, t), \tag{2.1}$$

$$\frac{\partial s}{\partial \beta} \equiv \frac{\partial s}{\partial t} + (V-a)\frac{\partial s}{\partial x} = \frac{a}{2c_p(k-1)}\frac{\partial S}{\partial \beta} - \frac{a}{2}\frac{D\ln A}{Dt} + G(a, V, x, t), \tag{2.2}$$

where

$$r = \frac{a}{k-1} + \frac{V}{2}, \quad s = \frac{a}{k-1} - \frac{V}{2},$$

a denotes the velocity of sound, V the velocity of flow, α and β the curvilinear characteristic co-ordinates, S the specific entropy, and A the cross-section area

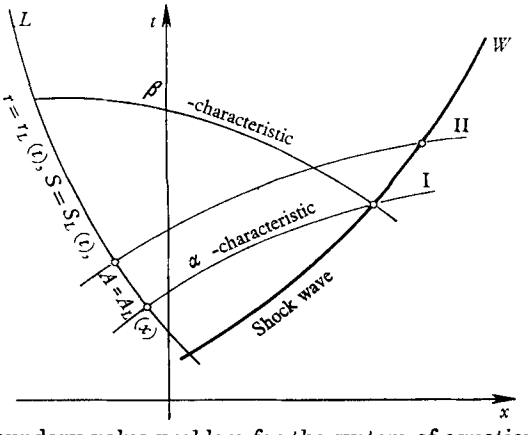

FIGURE 1. The boundary-value problem for the system of equations (2.1) and (2.2).

measured along plane, cylindrical or spherical surfaces for the cases of approximately cylindrical, wedge-shaped or conical ducts, respectively.

$$\frac{D}{Dt} = \frac{\partial}{\partial t} + V\frac{\partial}{\partial x}$$

is the substantial derivative, and F and G are coefficients which express the entropy change of an element of the gas and the cross-outflow influence on the mass and momentum equations.† The boundary-value problem for the above system of differential equations can be set as follows. In the (x, t)-plane, suppose the line L, not a characteristic, is given (see figure 1) and that on this line values

* In an as yet unpublished paper the author has applied similar methods to the calculation of the shock-wave shape and pressure distribution for hypersonic flow around bodies of revolution.

† See §5.

$r = r_L(t)$, $S = S_L(t)$ and $A = A_L(x)$ are known. On the right of a second unknown line (the shock wave) the state of the gas is prescribed by $V_1 = V_1(x)$, $a_1 = a_1(x)$ and $S_1 = S_1(x)$. Along this line compatibility conditions must be fulfilled. These conditions connect the parameters ahead of the shock wave (suffix 1) with parameters on the back of the shock wave (suffix W), and can be written in the form

$$\bar{V}_W = \frac{2}{k+1}\left(\bar{W}_1 - \frac{1}{\bar{W}_1}\right) + \bar{V}_1, \tag{2.3}$$

$$\bar{a}_W = \frac{1}{k+1}\sqrt{\left[2(k-1)\left(k\bar{W}_1^2 - \frac{1}{\bar{W}_1^2}\right) + 6k - k^2 - 1\right]}, \tag{2.4}$$

$$r_W \equiv f(\bar{W}_1, \bar{V}_1, a_1) = \left(\frac{\bar{a}_W}{k-1} + \frac{\bar{V}_W}{2}\right) a_1, \tag{2.5}$$

$$S_W \equiv \phi(\bar{W}_1, S_1) = c_V \ln\left\{\left[\frac{2k}{k+1}\bar{W}_1^2 - \frac{k-1}{k+1}\right]\left[\frac{(k-1)\bar{W}_1^2 + 2}{(k+1)\bar{W}_1^2}\right]^k\right\} - S_1, \tag{2.6}$$

where
$$\bar{W}_1 = \frac{U - V_1}{a_1}, \quad \bar{V}_W = \frac{V_W}{a_1}, \quad \text{etc.}, \tag{2.7}$$

and U is the velocity of propagation of the shock wave.

We suppose that $A = A(x)$. Then equation (2.1) can be written in the form

$$\frac{\partial r}{\partial \alpha} - \frac{a}{2c_p(k-1)}\frac{\partial S}{\partial \alpha} + \frac{aV}{2(V+a)}\frac{\partial \ln A}{\partial \alpha} = F(a, V, \alpha, \beta). \tag{2.8}$$

Integrating equation (2.8) along α-characteristics (see figure 1) and expressing the values on the shock wave by equations (2.5) and (2.6), we obtain*

$$f(\bar{W}_1, V_1, a_1) - r_L - \int_{S_L}^{\phi(\bar{W}_1, S_1)} \frac{a}{2(k-1)c_p}\, dS + \int_{\ln A_L}^{\ln A_W} \frac{aV}{2(V+a)}\, d\ln A = \int_{\alpha_L}^{\alpha_W} F(a, V, x, t)\, d\alpha,$$

where the suffix L refers to values of the parameters on the L-line. We now apply this expression to two neighbouring characteristics I and II (see figure 1). On subtracting these expressions, we obtain in the limit as characteristic I approaches characteristic II,†

$$f'_{\bar{W}_1}(\bar{W}_1, V_1, a_1)\, d\bar{W}_1 + f'_{V_1}(\bar{W}_1, V_1, a_1)\, dV_1 + f'_{a_1}(\bar{W}_1, V_1, a_1)\, da_1 - dr_L - \left[\frac{a}{2(k-1)c_p}\right]_W \times [dS_1 + \phi'_{\bar{W}_1}(\bar{W}_1, S_1)\, d\bar{W}_1] + \left[\frac{a}{2(k-1)c_p}\right]_L dS_L - \left[\frac{1}{2(k-1)c_p}\, da\right]_m [\phi(\bar{W}_1, S_1) - S_L] + \left[\frac{aV}{2(V+a)}\right]_W d\ln A_W - \left[\frac{aV}{2(V+a)}\right]_L d\ln A_L + \frac{1}{2}\left[d\left(\frac{aV}{V+a}\right)\right]_m \ln\frac{A_W}{A_L} = F_W d\alpha_W - F_L d\alpha_L + [dF]_m(\alpha_W - \alpha_L),$$

where the suffix m refers to the mean value in the interval considered.

* $\int_{\alpha_L}^{\alpha_W} \frac{\partial r}{\partial \beta}\, d\beta = 0$, etc., because $d\beta = 0$ along α-characteristics.

† From equation (2.6) we have $\phi'_{S_1}(\bar{W}_1, S_1) = 1$.

For the case when the variations of the flow behind the shock wave are small (the linearized case), all values can be written as $A = A_L + \epsilon_A$, $a = a_L + \epsilon_a$, etc., where $\epsilon_A \ll A_L$, $\epsilon_a \ll a_L$, etc. We can then omit in the above equation as small quantities of the second order all the terms in which the suffix m appears. Then we obtain

$$f'_{\overline{W}_1}(\overline{W}_1, V_1, a_1)\,d\overline{W}_1 + f'_{V_1}(\overline{W}_1, V_1, a_1)\,dV_1 + f'_{a_1}(\overline{W}_1, V_1, a_1)\,da_1$$
$$-\left[\frac{a}{2(k-1)c_p}\right]_W [dS_1 + \phi'_{\overline{W}_1}(\overline{W}_1, S_1)\,d\overline{W}_1] + \left[\frac{aV}{2(V+a)}\right]_W d\ln A_W - F_W d\alpha_W$$
$$= dr_L - \left[\frac{a}{2(k-1)c_p}\right]_L dS_L + \left[\frac{aV}{2(V+a)}\right]_L d\ln A_L - F_L d\alpha_L. \qquad (2.9)$$

For the general case we may use the formula (2.9) as an approximation.

The same procedure can be carried out with the formula analogous to (2.8) for the β-characteristics. In this manner we could obtain in addition the value of $s_L = a_L/(k-1) - \frac{1}{2}V_L$ along the L-line. The main difficulty is to find the points of intersection of corresponding characteristics with the W-line and the L-line. For this purpose an additional assumption is necessary (see § 6 B below). Often, instead of $r_L(t)$, the value of $V_L(t)$ (for example, the piston velocity) is given along the L-curve. In this case, the value of $r_L(t)$ depends on $s_L(t)$, which can be found only if the distribution of $r_L(t)$ is known. The situation is now more complicated. This kind of boundary condition occurs in the problem of variable piston motion behind the shock wave, when the reflected wave reaches the piston. This problem was solved by Gundersen (1958), but only in the linearized approximation for small variations of the piston velocity when all the flow field can be found in closed form.*

In the special case of boundary conditions such that $r_L = \text{const.}$, $S_L = \text{const.}$, $A_L = A_0 = \text{const.}$, we obtain from (2.9) Whitham's characteristic rule. In the case of $F = 0$ and constant state ahead of the shock wave, this rule can be written in the form

$$f'_U dU - \frac{a_W}{2c_p(k-1)}\phi'_U dU + \left[\frac{aV}{2(V+a)}\right]_W d\ln\frac{A_W}{A_0} = 0.$$

Whitham obtained this rule in a different way: he made use of the equation (2.1), in which he replaced derivatives in the characteristic direction by derivatives in the shock-wave direction $\{\partial/\partial\gamma = \partial/\partial t + U(\partial/\partial x)\}$. He remarks that the slope of the α-characteristics is close to that of the shock-wave line (in the linearized approximation, they are the same).

The same result can be obtained (see Chisnell 1957 and Rościszewski 1958) by solving first the linearized case for small shock-wave velocity variations, and then, for the case of arbitrarily variable shock-wave velocity, changing the parameter in the linearized solution. The quasi-linearized solution obtained in

* In the general case it is necessary to make use of the expression analogous to (2.9) for β-characteristics. Unknown β-characteristics could be replaced by characteristics taken from the simple wave solution. In the analogous case discussed in the author's unpublished work dealing with hypersonic flow around bodies of revolution, a similar method shows good accuracy.

this way is, in fact, the result of applying a series of local linearized solutions to the case where finite changes in shock-wave velocity takes place.

The formula (2.9) will be applied below to many different cases of non-uniform shock-wave motion. The results will be compared diagrammatically with finite difference calculations obtained from the method of characteristics; these comparisons display the surprisingly good accuracy of the present method.

A similar boundary-value problem will later be formulated for plane steady supersonic flow (see § 8).

3. Shock-wave propagation in a duct of non-uniform cross-section

We shall now apply the rule to the case of shock-wave motion in a tube in which the cross-section is initially constant and then varies, and for which there is a given constant state ahead of the shock wave (see figure 2). In particular, shock-wave propagation in ducts of variable cross-section, when the gas ahead of the shock wave is in steady motion or at rest with a variable temperature field, can be considered.

We suppose that $A = A(x)$ and neglect the heat exchange and surface friction ($F = 0$). In the case considered, along the t-axis we have $r = \text{const.}$ and $A = A_0$ (see figure 2). Taking the t-axis as an L-line, we have $dr_L = 0$, $dA_L = 0$, $dS_L = 0$. Now taking a_1, V_1, S_1 as variable, and dividing equation (2.9) by dx, we obtain, using equation (2.7),

$$\frac{dU}{dx} = \left(1 - \frac{1}{2N}\right)\frac{dV_1}{dx} - \left(\overline{V}_1 - \overline{U} + \frac{\bar{r}_W - \frac{1}{2}\overline{V}_1}{N}\right)\frac{da_1}{dx} + \frac{a_W}{2(k-1)c_p N}\frac{dS_1}{dx} - \frac{V_W a_W}{2N(V_W + a_W)}\frac{d\ln(A/A_0)}{dx}, \tag{3.1}$$

where

$$N = R - \frac{\bar{a}_W E}{2(k-1)}, \tag{3.2}$$

$$R = f'_{\overline{W}_1}(\overline{W}_1, V_1, a_1) = \frac{1}{k+1}\left[\frac{2k\overline{W}_1 + (2/\overline{W}_1^3)}{(k+1)\bar{a}_W} + 1 + \frac{1}{\overline{W}_1^2}\right], \tag{3.3}$$

$$E = \phi'_{\overline{W}_1}(\overline{W}_1, S_1)\frac{1}{c_p} = \frac{4\overline{W}_1}{2k\overline{W}_1^2 - k + 1} - \frac{4}{\overline{W}_1[(k-1)\overline{W}_1^2 + 2]}. \tag{3.4}$$

For the given state ahead of the shock wave, dV_1/dx, da_1/dx, and dS_1/dx are known functions of x, and the equation (3.1) is a first-order differential equation for $U = U(x)$. In general this equation can be quite easily solved numerically; then we obtain the unknown shock wave without having to solve the partial differential equations. In the special case of an approximately cylindrical duct and small variations of the values of the flow parameters ahead of the shock wave, all the coefficients of equation (3.1) can be taken, according to the linearized approximation, as constant. Therefore, a closed-form solution can be obtained for the shock-wave velocity change and the entire field on the back of the shock wave. The discussion of this solution was given in the author's previous work (Rościszewski 1958).

In the more general case when the time-dependent field ahead of the shock wave is given [$V_1 = V_1(x,t)$, $a_1 = a_1(x,t)$, $S_1 = S_1(x,t)$] and, as before, $dr_L = 0$, $dA_L = 0$, $dS_L = 0$, in place of d/dx on the right-hand side of equation (3.1) we must put $\partial/\partial x + (1/U)(\partial/\partial t)$. We then obtain the equation for the shock-wave velocity in the form

$$\frac{dU}{dx} = F(U,x,t) \equiv F\left(U, x, \int_0^x \frac{dx}{U}\right).$$

This equation can also easily be solved numerically.

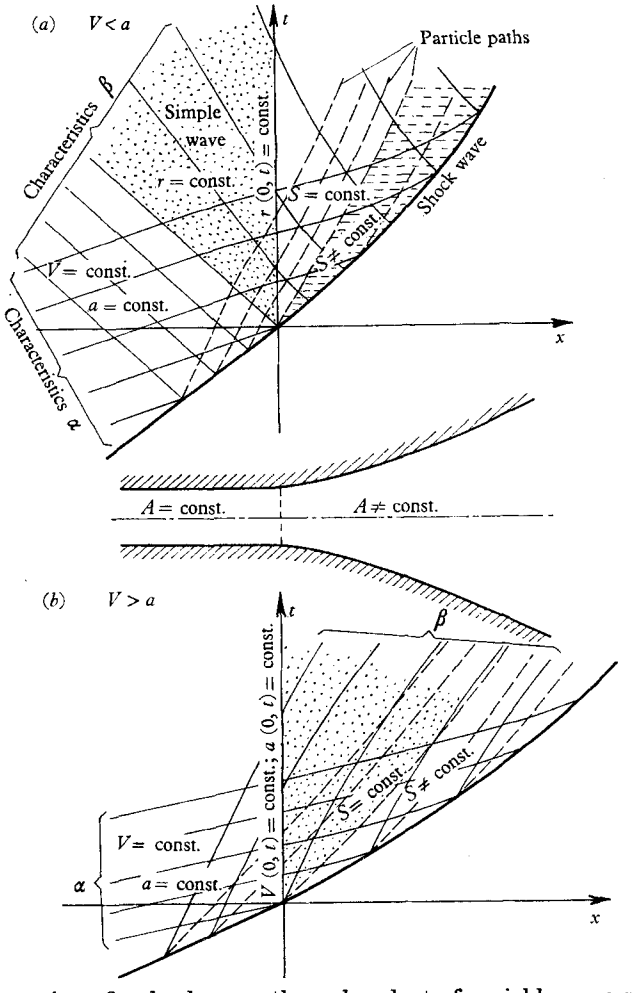

FIGURE 2. Propagation of a shock wave through a duct of variable cross-section, (*a*) subsonic flow behind the shock wave, (*b*) supersonic flow behind the shock wave.

The solution of the problem when time-dependent boundary conditions on curve L are given [$r_L = r_L(t)$, $A_L = A_L(t)$] is also possible, and it is not very complicated when the curve L lies outside the domain of dependence bounded by the β-characteristic and the shock wave, i.e. when the condition on the L-curve does not depend on the shock-wave motion.

In the special case when $a_1 = a_0 = \text{const.}$, $V_1 = 0$, $S_1 = \text{const.}$, using equations (2.3)–(2.6) we obtain from equation (3.1),

$$\ln\frac{A}{A_0} = -\int_{\overline{U}_0}^{U}\left\{\frac{2(k+1)}{\sqrt{\{2(k-1)[k\overline{U}^2-(1/\overline{U}^2)]+6k-k^2-1\}}}+\frac{k+1}{\overline{U}-(1/\overline{U})}\right\}\times\left\{R-\frac{\overline{a}_W E}{2(k-1)}\right\}d\overline{U}, \quad (3.5)$$

where R and E are functions of $\overline{U}$ given by equations (3.3) and (3.4).

$\overline{U}$	$-\int_2^{\overline{U}}\{\}\,d\overline{U}$	$\overline{U}$	$-\int_2^{\overline{U}}\{\}\,d\overline{U}$	$\overline{U}$	$-\int_2^{\overline{U}}\{\}\,d\overline{U}$
1·2	−4·514	3·5	3·186	5·8	5·817
1·3	−3·563	3·6	3·338	5·9	5·854
1·4	−2·612	3·7	3·481	6·0	5·991
1·5	−1·999	3·8	3·623	6·1	6·076
1·6	−1·490	3·9	3·757	6·2	6·160
1·7	−1·053	4·0	3·891	6·3	6·242
1·8	−0·668	4·1	4·017	6·4	6·323
1·9	−0·322	4·2	4·144	6·5	6·402
2·0	0·000	4·3	4·265	6·6	6·482
2·1	0·294	4·4	4·385	6·7	6·559
2·2	0·587	4·5	4·501	6·8	6·635
2·3	0·845	4·6	4·616	6·9	6·710
2·4	1·102	4·7	4·727	7·0	6·785
2·5	1·330	4·8	4·838	7·1	6·858
2·6	1·559	4·9	4·944	7·2	6·930
2·7	1·767	5·0	5·050	7·3	7·001
2·8	1·974	5·1	5·152	7·4	7·071
2·9	2·160	5·2	5·254	7·5	7·140
3·0	2·356	5·3	5·352	7·6	7·208
3·1	2·537	5·4	5·449	7·7	7·275
3·2	2·707	5·5	5·543	7·8	7·341
3·3	2·870	5·6	5·636	7·9	7·407
3·4	3·033	5·7	5·727	8·0	7·472

TABLE 1

In the limiting case when $\overline{U} \to \infty$ we obtain the asymptotic formula

$$\ln\frac{A}{A_0} = \left(\sqrt{\frac{2k}{k-1}}+1+\frac{2}{k}\right)\ln\frac{\overline{U}}{\overline{U}_0}. \quad (3.6)$$

In fact, equation (3.5) is the Chisnell answer presented in another form. Some numerical differences between Chisnell's tables and present formula are, however, found (see the converging cylindrical wave calculation). Values of the integral in (3.5) are given in table 1 for $k = 1{\cdot}4$.

Equation (3.4) enables us to examine the influence of entropy changes on shock-wave motion. The coefficient depends on

$$\frac{1}{c_p}\frac{d(S_W - S_1)}{d\overline{W}_1} = E,$$

where E given by equation (3.4) expresses the entropy change influence. When $\overline{W}_1 = 1$ (very weak shock wave) and $\overline{W}_1 = \infty$ (very strong shock wave) E vanishes. This means that entropy changes for hypersonic shock motion can be neglected. Table 2 gives values of E as a function of W_1 for $k = 1{\cdot}4$.

The results of calculations by the use of Table 1 are compared with step-by-step calculations* applied to the basic differential equations for various duct shapes and various initial shock strengths (figures 3–10). In special cases these

W	0	1·5	2	3	4	5	6	8	10	15	20	∞
E	0	0·097	0·185	0·246	0·241	0·221	0·198	0·161	0·123	0·092	0·0714	0

TABLE 2

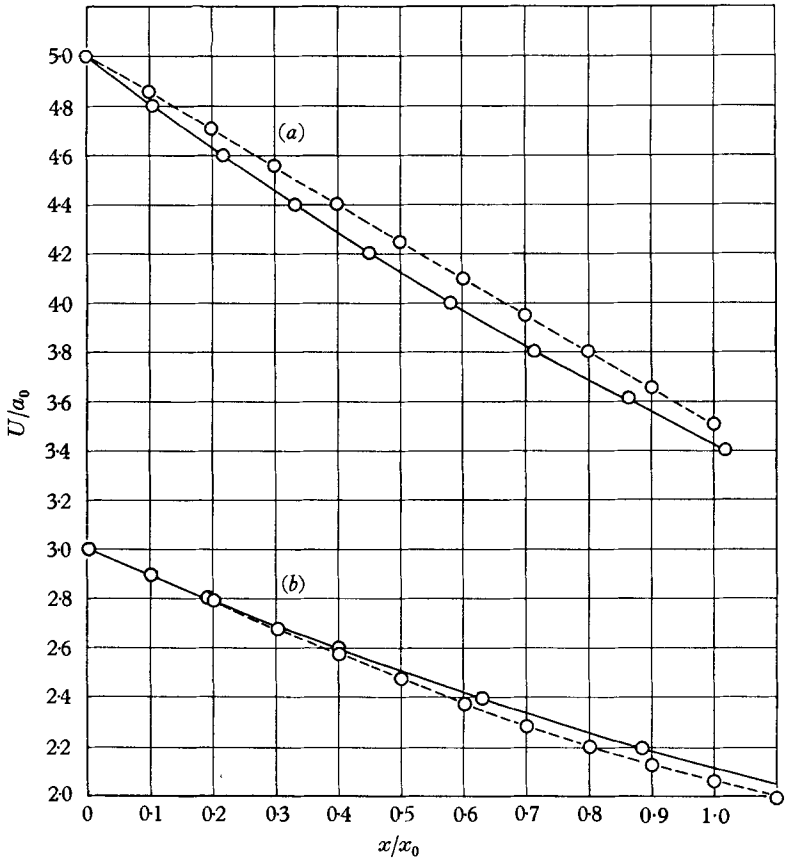

FIGURE 3. Comparison of the present method with step-by-step calculations by the method of characteristics for the case of shock-wave propagation through a duct of varying cross-section area given by $A/A_0 = e^{2(x/x_0)}$ (divergent duct) and initial shock strengths (*a*) $U_0/a_0 = 5$ and (*b*) $U_0/a_0 = 3$. The shock is assumed plane. – – – –, Step-by-step calculation; ——, present method.

* This calculation was based on the method of characteristics. The accuracy was checked by taking some mean characteristics which give the errors lying within the limits of accuracy of the wave diagram calculations.

results are compared (figure 9) with Payne's (1957) calculations for a cylindrical convergent wave. In this case, because of other boundary conditions (in Payne's work $V(1,t) \neq$ const.) Payne's results differ from those given by the present method and from those given by finite difference calculations by the method of

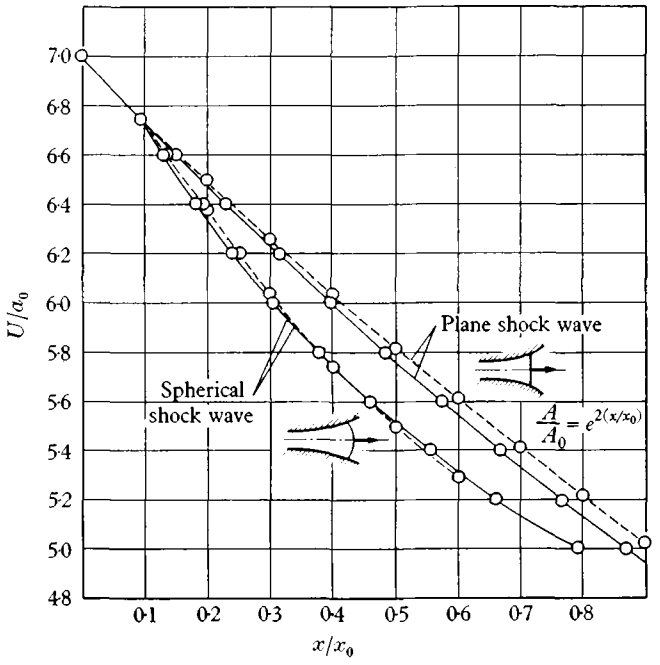

FIGURE 4. Comparison of the present method with calculations by the method of characteristics for the case of shock-wave propagation through a duct varying cross-section area given by $A/A_0 = e^{2(x/x_0)}$ (divergent duct) and initial shock strength $U_0/a_0 = 7$. The comparison is made for both a plane and spherical shock wave, originating at $x = 0$, for $x/x_0 > 0{\cdot}1$. ----, Step-by-step calculations; ——, present method.

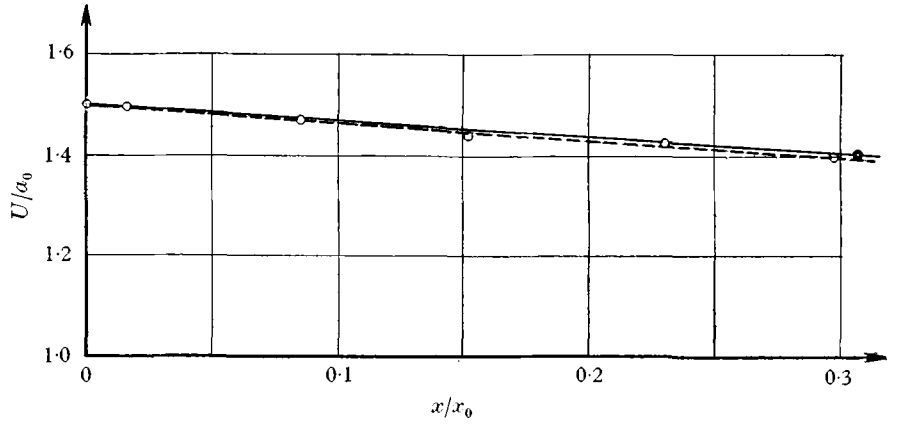

FIGURE 5. Comparison of the present method with calculations by the method of characteristics for the case of shock-wave propagation through a duct with $A/A_0 = e^{(x/x_0)}$ (divergent duct) and initial shock strength $U_0/a_0 = 1{\cdot}5$. ----, Step-by-step calculations; ——, present theory.

characteristics. The results are not strictly insensitive to the initial conditions, see Whitham (1958). Chisnell's tables show some disagreement with the present tables, and they give results very close to Payne's calculations for different

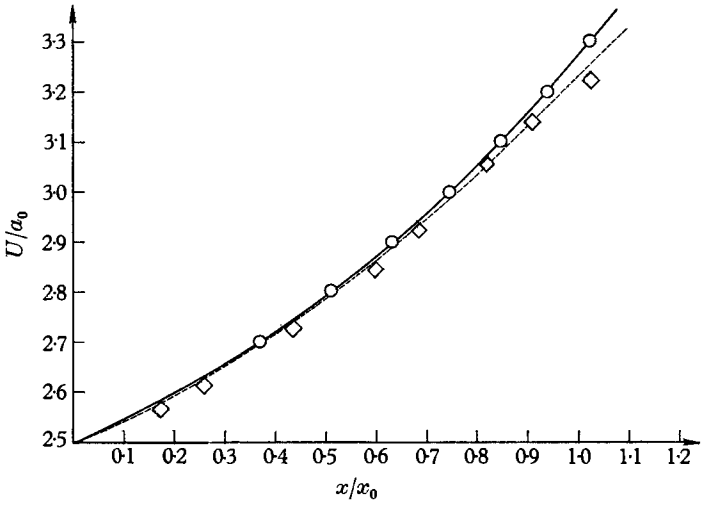

FIGURE 6. Comparison of the present method with calculations by the method of characteristics for the case of shock wave propagation through a duct with $\frac{A}{A_0} = \exp\left[-\left(\frac{x}{x_0}+\frac{x^2}{2x_0^2}\right)\right]$ (convergent duct) and initial shock strength $U_0/a_0 = 2{\cdot}5$. – – –, Step-by-step calculations; ——, present method.

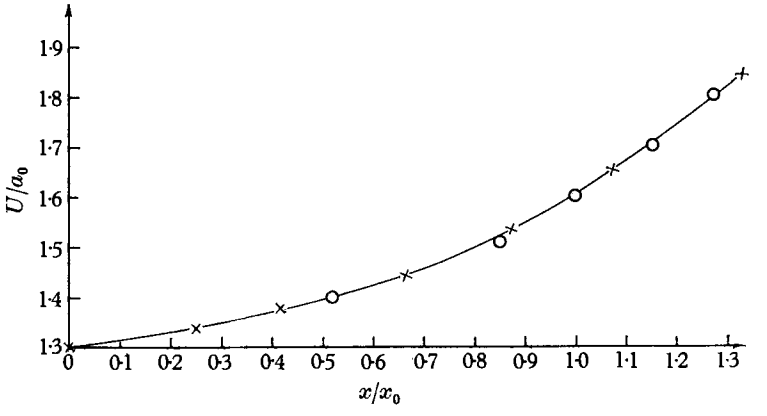

FIGURE 7. Comparison of the present method with calculations by the method of characteristics for the case of shock-wave propagation through a duct with $\frac{A}{A_0} = \exp\left[-\left(\frac{x}{x_0}+\frac{x^2}{2x_0^2}\right)\right]$ (convergent duct) and initial shock strength $U_0/a_0 = 1{\cdot}3$. ○, Step-by-step calculations; ×, present theory.

boundary conditions. For other cases calculated in this paper, Chisnell's tables also show some deviations. Results of the comparison of the present method with experimental results and calculations by Hertzberg & Kantrowitz (1950) are given in figure 10.

4. Propagation of strong detonation wave through ducts of non-uniform cross-section

Here we shall be concerned with the propagation of a strong detonation wave, i.e. the detonation wave described by the points on the Hugoniot curve lying above the Chapman–Jouguet point (see Courant & Friedrichs 1948). Such a detonation wave can be obtained by additional compression behind the detonation wave, for example, by piston motion or by the propagation of the Chapman–

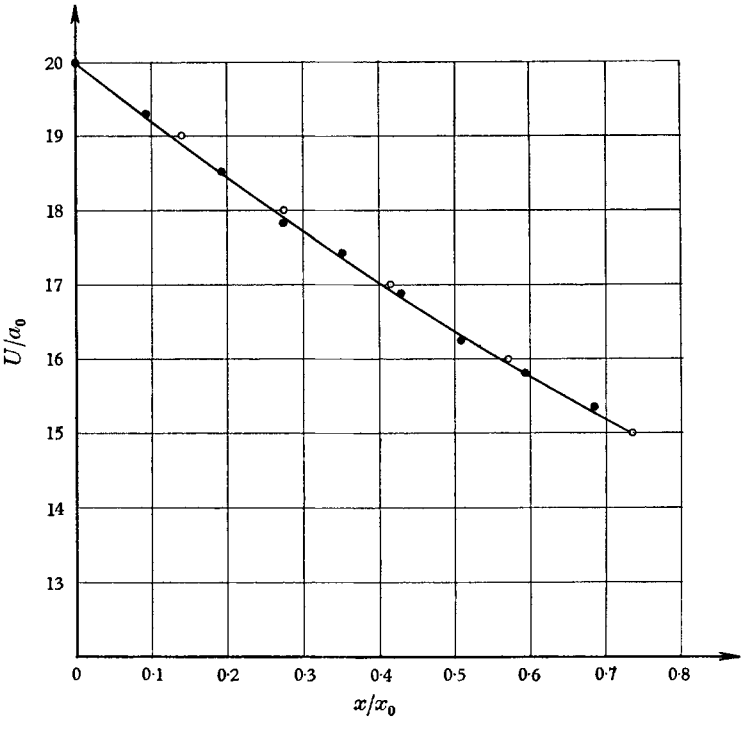

FIGURE 8. Comparison of the present method with calculations by the method of characteristics for the case of a very strong shock wave ($U_0/a_0 = 20$) propagating through a duct of variable cross-section $A/A_0 = e^{2(x/x_0)}$. The gas is treated as ideal with $k = 1{\cdot}4$. ●, Step-by-step calculations; ○, present method.

Jouguet detonation wave through a duct of suddenly convergent cross-section. We assume the strong detonation wave to be propagated through a duct of initially constant cross-section, which at some point changes into a duct with variable cross-section. The gas ahead of the detonation wave is assumed to be at rest with a constant velocity of sound.

In a divergent duct the velocity of a detonation wave can be decreased only to that corresponding to the Chapman–Jouguet wave. The only difference between the solution of the previous case and the present one is in the different compatibility equations for shock and detonation waves.

We assume different values of $k = c_p/c_v$ in front (suffix 1) and at the back (suffix W) of the detonation wave.

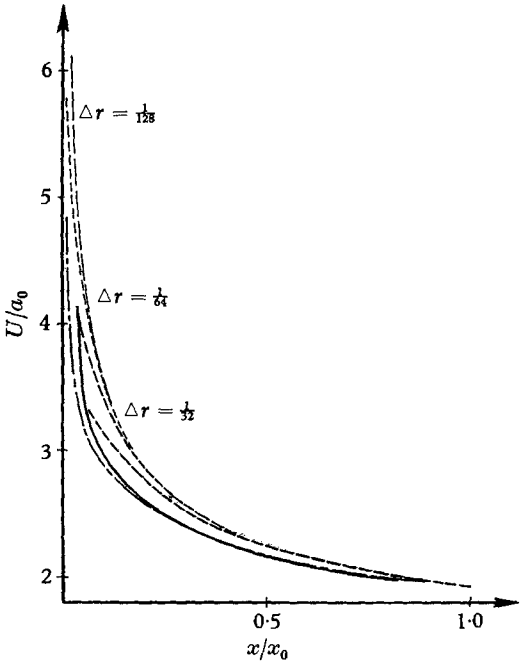

FIGURE 9. Comparison of the present method with calculations by the method of characteristics (assuming $V(1, t) = \text{const.}$) and Payne's calculations with different boundary conditions ($V(1, t) \neq \text{const.}$). —·—·—, Step-by-step calculations with boundary condition $V(1, t) = \text{const.}$; – – –, finite difference calculations by Payne $V(1, t) \neq \text{const.}$; ——, present method; ——, Chisnell (published in Payne's work).

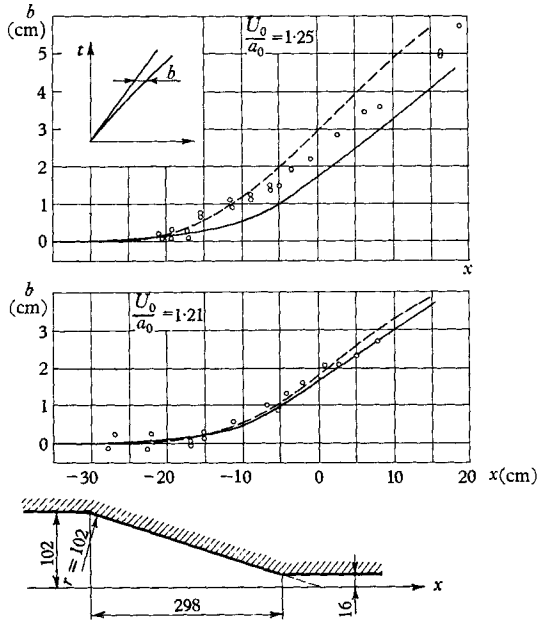

FIGURE 10. Comparison of the present method with Hertzberg & Kantrowitz's experimental curve and their calculations by the method of characteristics. ○, Experimental points (Hertzberg–Kantrowitz); – – –, finite difference calculations (Hertzberg–Kantrowitz); ——, present method.

The equations of conservation of mass, momentum and energy (see Courant & Friedrichs 1948) give

$$\bar{V} = \frac{1}{k_2+1}\left(\bar{U} - \frac{k_2}{k_1}\frac{1}{\bar{U}}\right) + \sqrt{\left\{\left(\bar{U} - \frac{k_2}{k_1}\frac{1}{\bar{U}}\right)\frac{1}{(k_2+1)^2} + \frac{2(k_2-1)Q}{(k_2+1)a_0^2} + \frac{2(k_1-k_2)}{k_1(k_1-1)(k_2+1)}\right\}}, \tag{4.1}$$

where $\bar{U} = U/a_0$ and $V = V_W/a_0$; Q is the heat released by the combustion process. Also,

$$\bar{a} = \sqrt{\left\{k_2(\bar{U}-\bar{V})\left(\bar{V} + \frac{1}{k_1\bar{U}}\right)\right\}}, \tag{4.2}$$

$$\frac{\Delta S}{c_p} = \frac{1}{k_2}\ln\bar{a} - \frac{k_2-1}{k_2}\ln\frac{\bar{U}}{\bar{U}-\bar{V}}, \tag{4.3}$$

where $\bar{a} = a_W/a_0$.

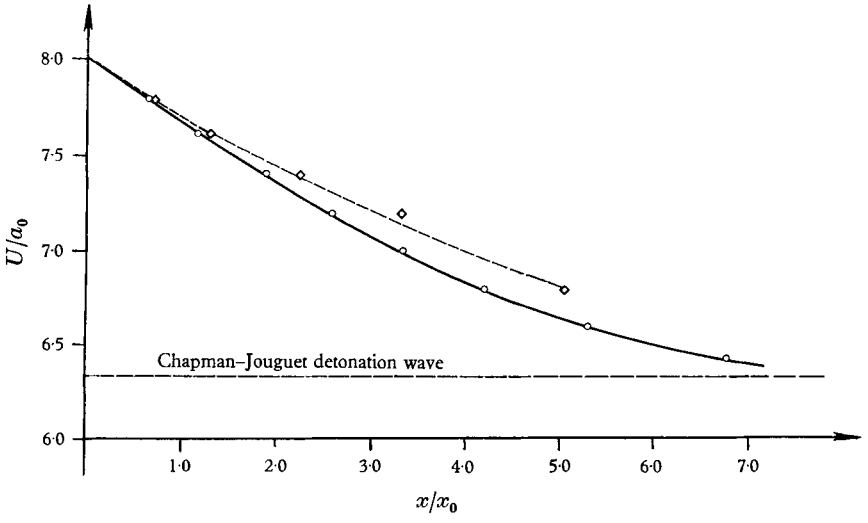

FIGURE 11. Comparison of the present method with calculations by the method of characteristics for the case of propagation of a strong detonation wave in a duct of cross-section given by $A/A_0 = e^{2(x/x_0)}$, with $k_1 = 1{\cdot}4$, $k_1 = 1{\cdot}3$ and $Q/a_0^2 = 28{\cdot}3$. ○, Present method; ◇, step-by-step calculations.

From equation (2.9) ($dV_1 = da_1 = dS_1 = 0$) we obtain

$$\ln\frac{A}{A_0} = \int_{\bar{U}_0}^{\bar{U}} \frac{2(\bar{V}+\bar{a})}{\bar{V}\bar{a}}\left\{\frac{1}{2}\frac{d\bar{V}}{d\bar{U}} + \frac{1}{k_2-1}\left(\frac{\partial\bar{a}}{\partial\bar{U}} + \frac{\partial\bar{a}}{\partial\bar{V}}\frac{d\bar{V}}{d\bar{U}}\right) - \frac{\bar{a}}{2(k_2-1)c_p}\left[\frac{\partial S}{\partial\bar{U}} + \frac{\partial S}{\partial\bar{V}}\frac{d\bar{V}}{d\bar{U}} + \frac{\partial S}{\partial\bar{a}}\left(\frac{\partial\bar{a}}{\partial\bar{U}} + \frac{\partial\bar{a}}{\partial\bar{V}}\frac{d\bar{V}}{d\bar{U}}\right)\right]\right\} d\bar{U}, \tag{4.4}$$

where the derivatives in equation (4.4) can be calculated by the use of equations (4.1), (4.2) and (4.3).

Comparison of the calculations by the use of the present method and step-by-step calculations are given in figure 11 for $k_1 = 1{\cdot}4$, $k_2 = 1{\cdot}3$ and $Q/a_0^2 = 28{\cdot}9$.

5. Shock-wave propagation through a duct with porous walls

In this section we consider the shock-wave attenuation due to the cross-outflow through porous walls of the duct. We take a cylindrical duct and we assume the cross mass flow $\pi d_0 l \rho \bar{v}$ to be small in comparison with $\rho V A$, where v is the cross-flow velocity, η is the ratio of the area of the pores to the area of the wall, and $\bar{v} = v\eta$.

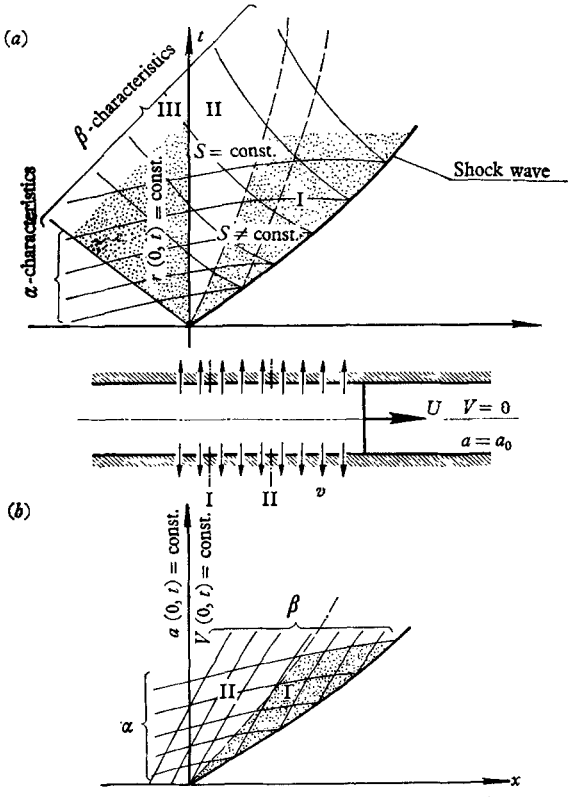

FIGURE 12. Flow induced by shock-wave propagation through a duct with porous walls ($\eta \ll 1$). (*a*) The case $V^0 < a^0$; (*b*) the case $V^0 > a^0$.

We apply the basic mechanical equations to the ideal flow through the duct with the porous wall (figure 12). We assume all parameters to be constant in the given cross-section. The continuity equation is

$$\rho_{\mathrm{I}} V_{\mathrm{I}} A_0 - \rho_{\mathrm{II}} V_{\mathrm{II}} A_0 - \pi d_0 \int_{x_{\mathrm{I}}}^{x_{\mathrm{II}}} \rho \bar{v}\, dx = \frac{\partial}{\partial t} \int_{x_{\mathrm{I}}}^{x_{\mathrm{II}}} \rho A_0\, dx,$$

or for $x_{\mathrm{I}} \to x_{\mathrm{II}}$

$$\frac{D\rho}{Dt} + \rho \frac{\partial V}{\partial x} = -\frac{4\rho\bar{v}}{d_0}. \tag{5.1}$$

For the momentum equation, we assume that the cross-stream has no momentum in the direction of the axis of the tube. Then we have

$$(p_{\mathrm{I}} - p_{\mathrm{II}}) A_0 + \rho_{\mathrm{I}} V_{\mathrm{I}}^2 A_0 - \rho_{\mathrm{II}} V_{\mathrm{II}}^2 A_0 = \frac{\partial}{\partial t} \int_{x_{\mathrm{I}}}^{x_{\mathrm{II}}} \rho V A_0\, dx,$$

or, using equation (5.1) for $x_{\mathrm{I}} \to x_{\mathrm{II}}$, we obtain

$$\frac{DV}{Dt} + \frac{1}{\rho}\frac{\partial p}{\partial x} = \frac{4V\bar{v}}{d_0}. \tag{5.2}$$

The energy equation is

$$\rho_{\mathrm{I}} V_{\mathrm{II}}\left(\frac{V_{\mathrm{I}}^2}{2} + \frac{k}{k-1}\frac{p_{\mathrm{I}}}{\rho_{\mathrm{I}}}\right) A_0 - \rho_{\mathrm{II}} V_{\mathrm{II}}\left(\frac{V_{\mathrm{II}}^2}{2} + \frac{k}{k-1}\frac{p_{\mathrm{II}}}{\rho_{\mathrm{II}}}\right) A_0 - \pi d_0 \int_{x_{\mathrm{I}}}^{x_{\mathrm{II}}} \rho\bar{v}\left(\frac{v^2}{2} + \frac{k}{k-1}\frac{p}{\rho}\right) dx$$

$$= \frac{\partial}{\partial t}\left[A_0 \int_{x_{\mathrm{I}}}^{x_{\mathrm{II}}} \rho\left(\frac{V^2}{2} + \frac{1}{k-1}\frac{p}{\rho}\right) dx\right],$$

or, using equations (5.1) and (5.2) for $x_{\mathrm{II}} \to x_{\mathrm{I}}$, we get

$$\frac{1}{c_p}\frac{DS}{Dt} = -\frac{2\bar{v}}{d}\left[(k-1)M^2 + \frac{k-1}{a^2}\bar{v}^2\right]. \tag{5.3}$$

We shall calculate the velocity of the cross-flow by assuming quasi-steady flow. This is based on the fact that due to a sudden change in the cross-section the local derivatives (in the equation of motion), are small in comparison with the convective terms. Then we apply the Bernoulli equation and assume the cross-flow to be isentropic

$$v = \zeta\sqrt{\left\{\frac{2k}{k-1}\frac{p}{\rho}\left[1 - \left(\frac{p_a}{p}\right)^{(k-1)/k}\right]\right\}} = \zeta\sqrt{\left\{\frac{2a^2}{k-1}\left[1 - \left(\frac{p_a}{p}\right)^{(k-1)/k}\right]\right\}}, \tag{5.4}$$

where $p_a = \text{const.}$ is the outside pressure, $p = p(x, t)$ is the pressure in the duct, and ζ is the loss coefficient.

The pressure in this formula can be calculated from

$$\frac{p}{p_2^0} = \left(\frac{a}{a_2^0}\right)^{2k/(k-1)} \exp\left(\frac{S_2^0 - S}{c_p - c_v}\right). \tag{5.5}$$

Taking into account the three equations of motion (5.1), (5.2), (5.3) and equation (5.4) we find the coefficients in equations (2.1) and (2.2) which express the entropy change and the cross-mass flow influence

$$F = -\frac{2a^2\eta\zeta}{d_0}\sqrt{\left\{\frac{2}{k-1}\left[1 - \left(\frac{p_a}{p}\right)^{(k-1)/k}\right]\right\}}\left\{1 - M + \frac{k-1}{2}M^2 + \zeta^2\left[1 - \left(\frac{p_a}{p}\right)^{(k-1)/k}\right]\right\}, \tag{5.6}$$

$$G = -\frac{2a^2\eta\zeta}{d_0}\sqrt{\left\{\frac{2}{k-1}\left[1 - \left(\frac{p_a}{p}\right)^{(k-1)/k}\right]\right\}}\left\{1 + M + \frac{k-1}{2}M^2 + \zeta^2\left[1 - \left(\frac{p_a}{p}\right)^{(k-1)/k}\right]\right\}, \tag{5.7}$$

where $M = V/a$.

We obtain from (2.9), where we substitute $d\alpha_L = 0$ (the t-axis is taken as the L-curve) and

$$d\alpha_W - d\alpha_L = \frac{dx}{V_W + a_W},$$

$$\int_{\bar{U}_0}^{\bar{U}} \frac{d\bar{U}}{B(\bar{U})} = \int \eta\, dx, \tag{5.8}$$

where $$B(\bar{U}) = \frac{F_W}{(V_W + a_W)\left[R - \dfrac{\bar{a}_W E}{2(k-1)}\right]}.$$

E and R are given by (3.3) and (3.4), respectively. The integral of the left-hand side of equation (5.8) is given in table 3 for $k = 1.4$ and $\zeta = 1$.

In figure 13 a comparison of the present method with the numerical method of characteristics is given for $\eta = 0{\cdot}1$ and $\bar{U}_0 = 4$. In this case the numerical method was not very accurate.

$\bar{U}$	$\int_{\bar{U}_0}^{U} \frac{dU}{\overline{B(U)}}$	$\bar{U}$	$\int_{\bar{U}_0}^{\bar{U}} \frac{dU}{\overline{B(U)}}$	$\bar{U}$	$\int_{\bar{U}_0}^{\bar{U}} \frac{dU}{\overline{B(U)}}$
1·2	−2·775	3·6	0·755	6·0	1·295
1·4	−0·900	3·8	0·814	6·2	1·328
1·6	−0·425	4·0	0·870	6·4	1·360
1·8	−0·172	4·2	0·922	6·6	1·391
2·0	0·000	4·4	0·972	6·8	1·421
2·2	0·144	4·6	1·019	7·0	1·450
2·4	0·264	4·8	1·064	7·2	1·478
2·6	0·367	5·0	1·107	7·4	1·506
2·8	0·460	5·2	1·148	7·6	1·532
3·0	0·544	5·4	1·187	7·8	1·558
3·2	0·621	5·6	1·224	8·0	1·584
3·4	0·691	5·8	1·260		

TABLE 3

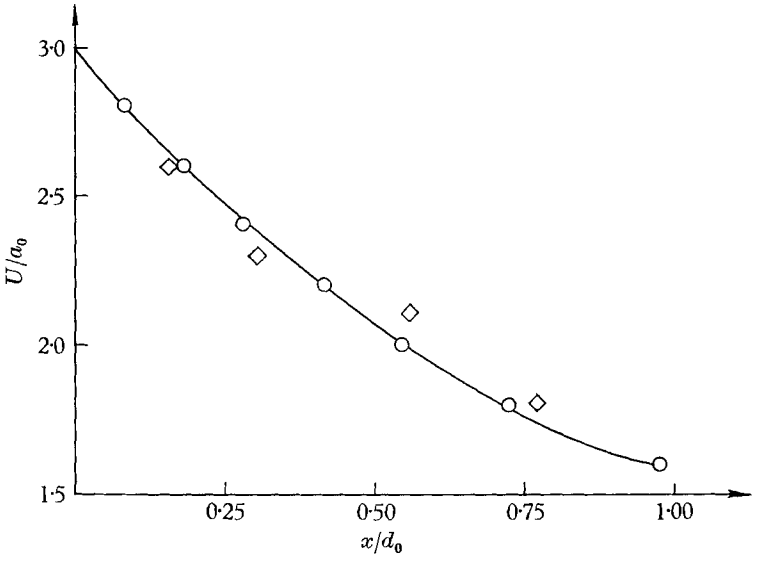

FIGURE 13. Comparison of the present method with the calculation by the method of characteristics for the case of shock-wave propagation through a duct with porous walls. The ratio of pore area to wall area $\eta = 0{\cdot}1$. Initial shock strength $U_0/a_0 = 4$. ◇, Step-by-step calculations; ○, present method.

6. Interaction of a rarefaction wave and a shock wave in one-dimensional unsteady flow

A. *Case of head-on collision*

Until now, these problems for arbitrary waves were solved by the use of finite difference methods. A discussion of these methods is given by Geiringer (1948).* We discuss the case of interaction of a simple wave and a shock wave of arbitrary strength (figure 14) in a duct of constant cross-section.† The flow behind the shock wave is governed by the unsteady non-isentropic flow equations.

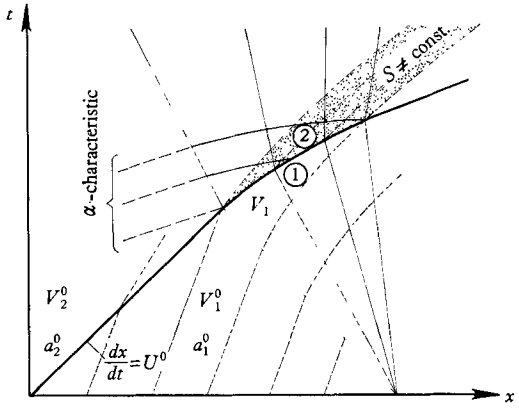

FIGURE 14. Head-on collision of a shock wave and simple rarefaction wave.

Introducing a simple wave relation ahead of the shock wave

$$da_1 = -\tfrac{1}{2}(k-1)\,dV_1, \tag{6.1}$$

and taking into account the fact that α-characteristics cross the uniform flow region behind the shock wave (see figure 13) ($dr_L = 0$), we get from equations (2.9) the first-order linear ordinary differential equation

$$\left[1-\frac{\chi(\overline{W}_1)+\frac{1}{2}(k-1)\,\overline{V}_1}{1+\frac{1}{2}(k-1)\,\overline{V}_1}\right]\frac{d\overline{V}_1}{d\overline{W}_1} = \psi(\overline{W}_1), \tag{6.2}$$

where from equations (2.4)–(2.7)

$$\chi(\overline{W}_1) = \frac{k-1}{k+1}\left(\overline{W}_1-\frac{1}{\overline{W}_1}\right)+\bar{a}_W, \tag{6.3}$$

$$\psi(\overline{W}_1) = \frac{\bar{a}_W}{k-1}E-\frac{2}{k+1}\left(1+\frac{1}{\overline{W}_1^2}\right)-\frac{4\left(k\overline{W}_1+\dfrac{1}{\overline{W}_1^3}\right)}{(k+1)^2\bar{a}_W}, \tag{6.4}$$

where $\bar{a}_W$ and E are given by (2.4) and (3.4) as a function of $\overline{W}_1$. Table 4 contains the values of $\chi(\overline{W}_1)$ and $\psi(\overline{W}_1)$ for $k = 1{\cdot}4$.

* The numerical example in this paper is incorrect. The principal equations of motion are not satisfied for the shock wave before interaction.

† This case is a special case of §3 when A = const. and $V_1 = V_1(x, t)$, etc., but we solve this here in a simpler manner.

The results for the special case of $V_1 = 0$ and $\overline{W}_1^0 = 4$ are compared in figure 15 with a step-by-step method of calculation (method of characteristics) applied to the basic non-linear partial differential equations. In this case the accuracy of the present method is excellent. The numerical calculations are very difficult because of the slow convergence of the finite difference method. Five iterations

$\overline{W}_1$	$\chi(\overline{W}_1)$	$\psi(\overline{W}_1)$	$\overline{W}_1$	$\chi(\overline{W}_1)$	$\psi(\overline{W}_1)$
1·0	1·00	3·32	4·6	2·92	1·58
1·2	1·11	2·82	4·8	3·10	1·58
1·4	1·21	2·50	5·0	3·22	1·57
1·6	1·32	2·28	5·2	3·33	1·56
1·8	1·43	2·12	5·4	3·44	1·55
2·0	1·54	2·00	5·6	3·56	1·54
2·2	1·65	1·90	5·8	3·68	1·54
2·4	1·76	1·84	6·0	3·80	1·53
2·6	1·86	1·77	6·2	3·92	1·53
2·8	1·98	1·72	6·4	4·03	1·52
3·0	2·08	1·69	6·6	4·15	1·52
3·2	2·19	1·66	6·8	4·27	1·51
3·4	2·30	1·64	7·0	4·38	1·51
3·6	2·41	1·63	7·2	4·51	1·50
3·8	2·52	1·62	7·4	4·63	1·50
4·0	2·64	1·61	7·6	4·74	1·49
4·2	2·76	1·60	7·8	4·86	1·49
4·4	2·88	1·59	8·0	4·98	1·48

TABLE 4

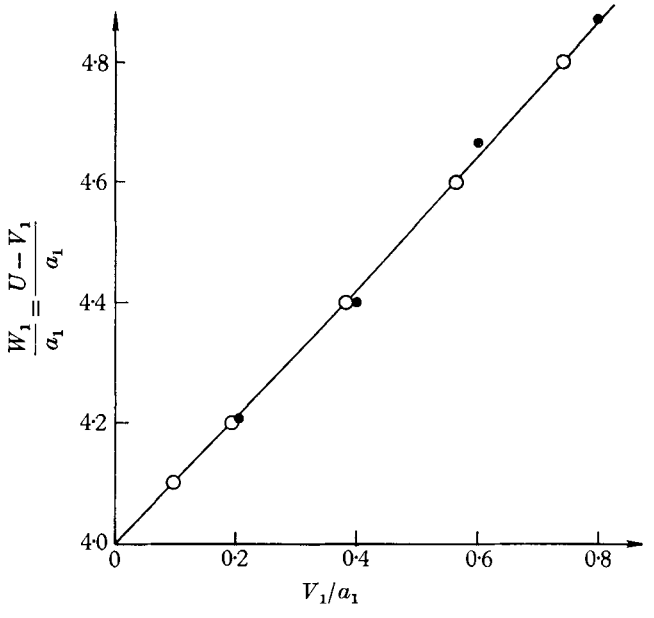

FIGURE 15. Comparison of the computation by use of the present method with the computation by the method of characteristics for the case of head-on collision of a shock wave of initial strength $W_1^0/a_1^0 = 4$ and a simple rarefaction wave. ●, Step-by-step calculations; ○, present method.

were made in each step for obtaining points of intersection of the characteristics α and the shock wave in the wave diagram; calculations in this case were then accurate.

B. *Case of the merging of a rarefaction and shock wave*

We consider the interaction of a rarefaction wave and a shock wave propagating in a duct of constant cross-section with a constant state ahead of the shock. Behind the shock wave is a piston which initially has a constant velocity (see figure 16).

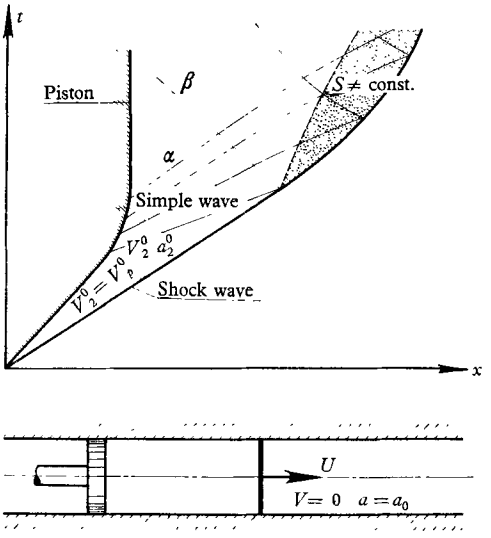

FIGURE 16. Merging of a shock wave and a rarefaction wave caused by non-uniform piston motion.

In the present case we have variable boundary conditions given on the arbitrary L-curve lying near the piston path. We assume that no reflexion wave going back from the shock wave reaches this curve.

Along the given curve we have the simple wave relation

$$s_L = \frac{a_L}{k-1} - \frac{V_L}{2} = \text{const.};$$

therefore

$$dr_L = dV_L = dV_p, \tag{6.5}$$

where V_p is the variable velocity in the simple wave prescribed by the piston motion.

Using equation (2.9) we obtain

$$d\bar{U}\left[R - \frac{\bar{a}_W E}{2(k-1)}\right] \equiv -\tfrac{1}{2}\psi(\bar{U})\,d\bar{U} = d\bar{V}_p, \tag{6.6}$$

where R and E are the functions of $\bar{U}$ given by equations (3.3) and (3.4).

After integrating we obtain the following equation

$$\frac{1}{2}\int_{\bar{U}^0}^{\bar{U}} \psi(\bar{U})\,d\bar{U} = \bar{V}_{p_2} - \bar{V}_{p_1}. \tag{6.7}$$

Table 5 contains values of the integral in equation (6.7) for $k = 1{\cdot}4$.

In this case the entropy change plays an essential role; and the shock expansion method does not give a good approximation. Equation (6.7) only enables the calculation of a change in the shock-wave velocity caused by the piston-velocity variation. To obtain the history of the shock-wave motion it is necessary to find the shape of the characteristics α.

$\bar{U}$	$\frac{1}{2}\int_{\bar{U}_0}^{\bar{U}} \psi(\bar{U})\, d\bar{U}$	$\bar{U}$	$\frac{1}{2}\int_{\bar{U}_0}^{\bar{U}} \psi(\bar{U})\, d\bar{U}$	$\bar{U}$	$\frac{1}{2}\int_{\bar{U}_0}^{\bar{U}} \psi(\bar{U})\, d\bar{U}$
1·2	−0·949	3·2	1·190	5·2	2·795
1·3	−0·806	3·3	1·274	5·3	2·872
1·4	−0·663	3·4	1·358	5·4	2·950
1·5	−0·543	3·5	1·441	5·5	3·027
1·6	−0·424	3·6	1·523	5·6	3·104
1·7	−0·314	3·7	1·605	5·7	3·181
1·8	−0·205	3·8	1·686	5·8	3·258
1·9	−0·102	3·9	1·767	5·9	3·335
2·0	0·000	4·0	1·848	6·0	3·412
2·1	0·098	4·1	1·928	6·1	3·488
2·2	0·196	4·2	2·008	6·2	3·565
2·3	0·290	4·3	2·088	6·3	3·641
2·4	0·385	4·4	2·167	6·4	3·718
2·5	0·477	4·5	2·246	6·5	3·794
2·6	0·568	4·6	2·325	6·6	3·870
2·7	0·707	4·7	2·404	6·7	3·947
2·8	0·847	4·8	2·483	6·8	4·023
2·9	0·923	4·9	2·561	6·9	4·069
3·0	1·020	5·0	2·639	7·0	4·115
3·1	1·105	5·1	2·717		

TABLE 5

On the basis of the step-by-step calculations it is observed that the α-characteristics are not very different from straight-lines.

Using these results we can calculate the change of the shock strength along the tube axis. Comparisons of the calculations by the present method and the finite difference method are given in figures 17–19 for various initial shock strengths and various modes of piston motion.

7. Interaction of a rarefaction wave and a contact surface in one-dimensional unsteady flow

The present method enables us to obtain in closed form the solution for the interaction of a rarefaction wave and a contact surface in an unsteady one-dimensional flow. In a similar way, the analogous problem in plane steady flow can be solved. Until now, the closed form solution only enabled the calculation of the finite value of the contact surface velocity (after interaction) to be done (see Billington 1956). The full history of the contact surface motion was obtained by step-by-step calculations (see Courant & Friedrichs 1948).

We assume the flow to be isentropic on the two sides of the contact surface (figure 20). The compatibility equations on the contact surface are

$$\left.\begin{aligned} V_{1c} &= V_{2c} = V_c, \\ p_{1c} &= p_{2c} = p_c \end{aligned}\right\} \tag{7.1}$$

(no velocity and pressure jump take place on the contact surface).

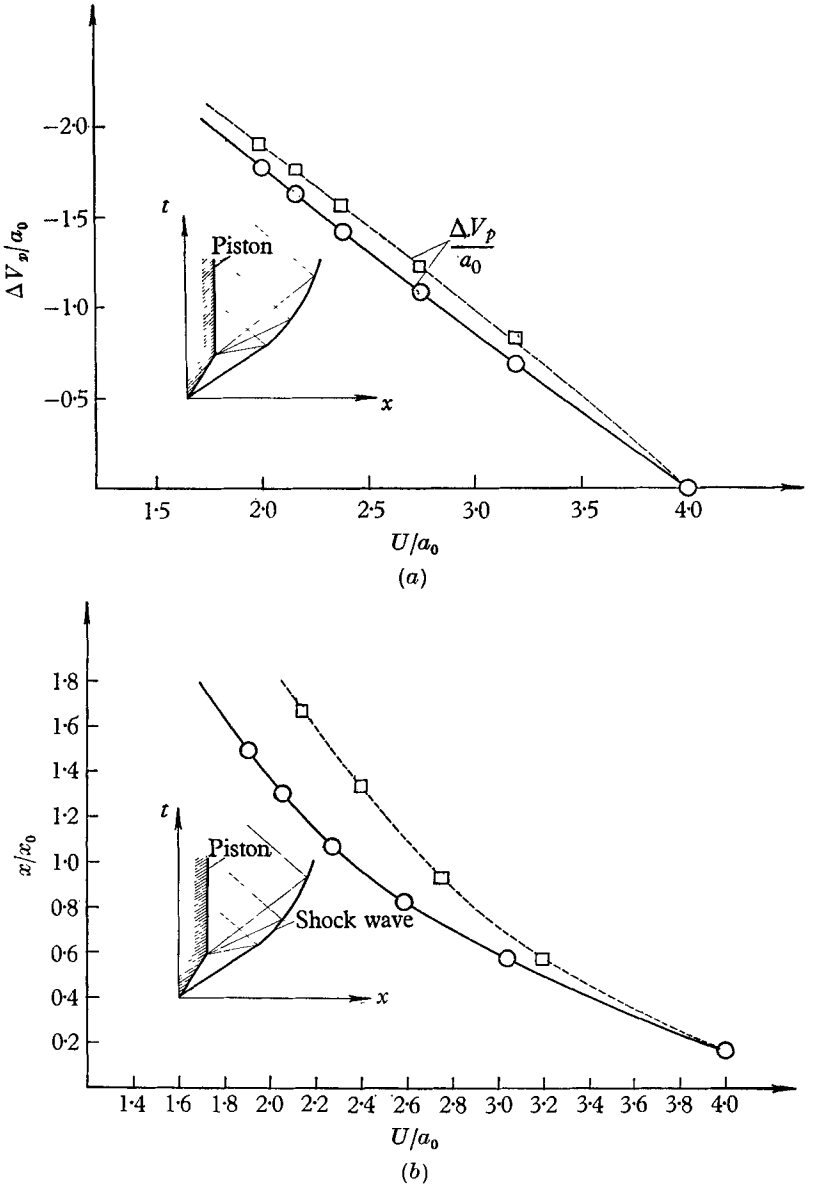

FIGURE 17. Comparison of the present method and calculations by the method of characteristics for the case of a shock wave of initial strength $U_0/a_0 = 4$ merging with a rarefaction wave caused by a suddenly stopped piston. (*a*) Shock-wave velocity versus piston velocity. (*b*) Change of the shock-wave propagation velocity, straight line α-characteristics being assumed. – – –, Step-by-step method; ——, present method.

From the second relation (7.1) and the equation of isentropic flow, we get

$$\left(\frac{a_{1c}}{a_1^0}\right)^{2k_1/(k_1-1)} = \left(\frac{a_{2c}}{a_2^0}\right)^{2k_2/(k_2-1)}, \tag{7.2}$$

where a_1^0, a_2^0 are the initial values of the velocity of sound on the right and left side of the contact surface.

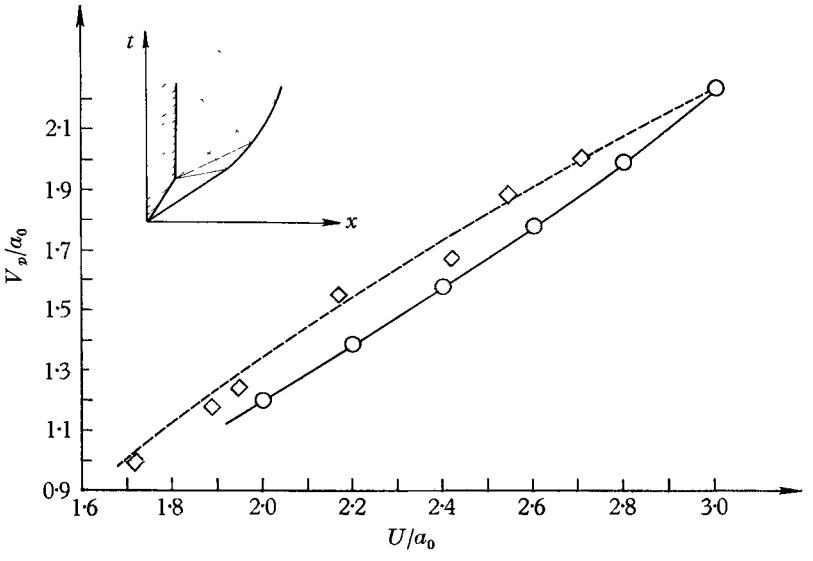

(*a*)

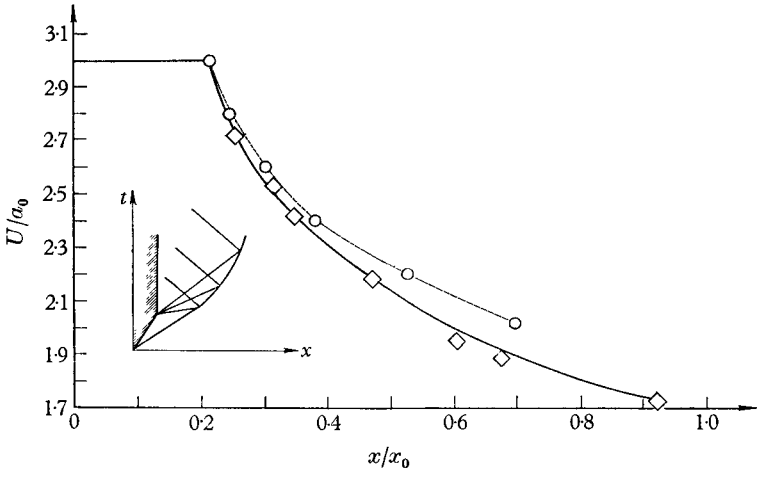

(*b*)

FIGURE 18. Comparison of the present method and calculations by the method of characteristics for the case of a shock wave of initial strength $U_0/a_0 = 3$ merging with a rarefaction wave caused by suddenly stopped piston. (*a*) Shock velocity versus piston velocity. (*b*) Change of the shock-wave propagation velocity, straight line α-characteristics being assumed. – – –, Step-by-step method; ——, present method.

We have $ds_1 = 0$ for the transmitted wave (simple wave) and therefore along the contact surface

$$\frac{a_{1c}}{k_1-1} - \frac{V_c}{2} = \frac{a^0_{1c}}{k_1-1} - \frac{V^0_c}{2}. \tag{7.3}$$

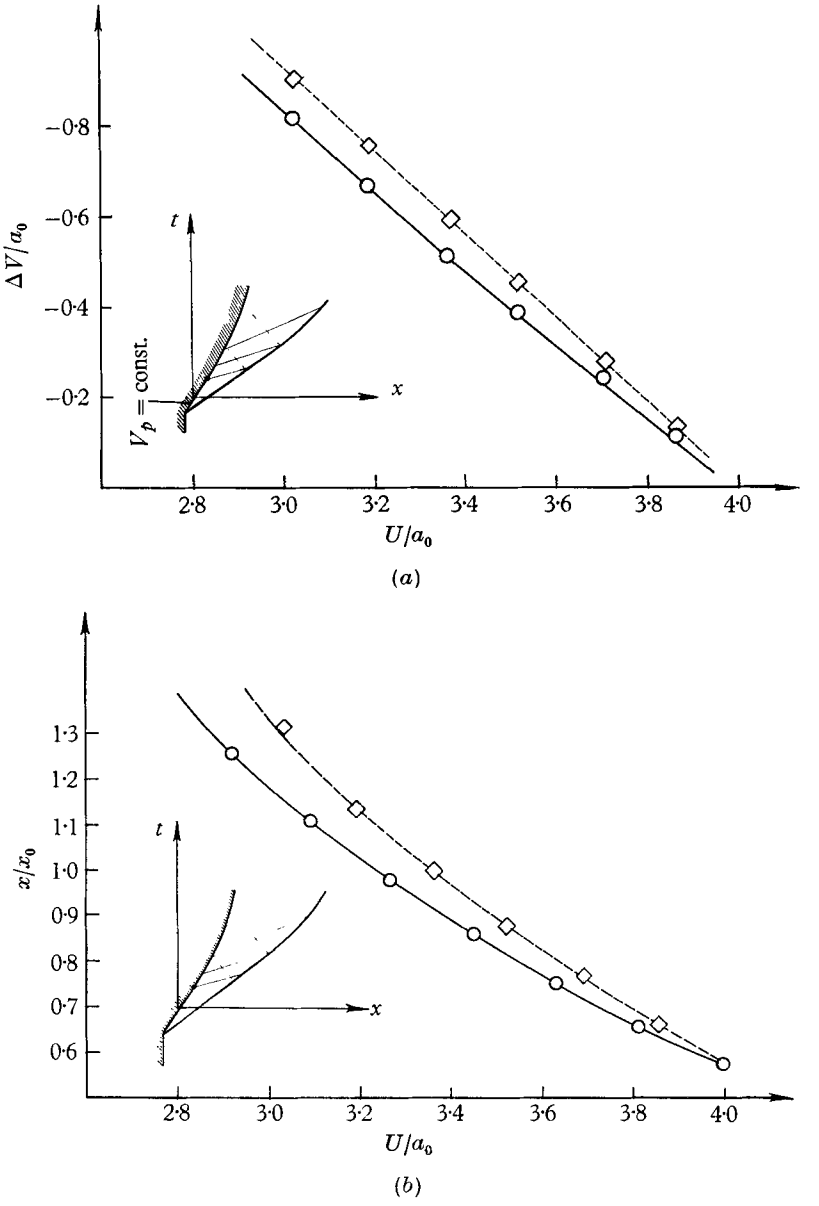

FIGURE 19. Comparison of the present method and calculations by the method of characteristics for the case of a shock wave of initial strength $U_0/a_0 = 4$ merging with a rarefaction wave caused by the retarded piston motion $dV_p/dt = W_p = -30(a_0/t_0)$. (*a*) Shock velocity versus piston velocity. (*b*) Change of the shock-wave propagation velocity, straight α-characteristics being assumed. – – – –, Step-by-step method; ——, present method.

For this case, in an analogous way to that leading to equation (2.9), we can write the following equation

$$dr_{2c} \equiv \frac{dV_c}{2} + \frac{da_{2c}}{k_2 - 1} = dr_L = dV_p. \tag{7.4}$$

Using equations (7.2) and (7.3) and integrating, we obtain the following expression

$$\frac{V_c - V_c^0}{2} + \frac{a_2^0}{k_2 - 1}\left[\frac{V_c - V_c^0}{2a_1^0}(k_1 - 1)\right]^{(k_2-1)/(k_1-1)(k_1/k_2)} = V_p - V_p^0. \tag{7.5}$$

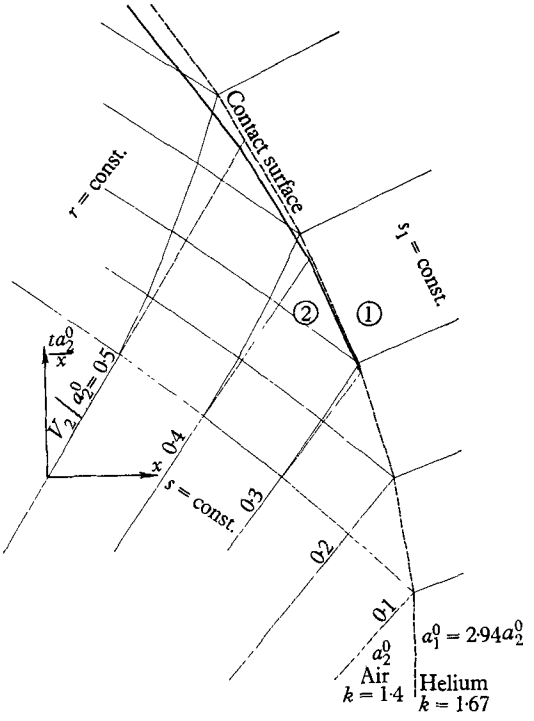

FIGURE 20. Time history of the interaction of a rarefaction wave with an air-helium contact surface, computed by the present method with the assumption of straight α-characteristics and by the method of characteristics. – – –, Step-by-step calculations; ——, present method.

This equation enables one to calculate the velocity of the contact surface for a given change in the simple wave velocity $V_p \equiv V_p(x/t)$. Assuming, as before in the case of the interaction of a rarefaction wave and a shock wave (see § 6B), that the α-characteristics are straight lines, we get the history of the contact surface motion. The results of the calculation are compared with the results of the method of characteristics and presented in figure 20 for an air-helium contact surface.

8. Wave interactions in plane steady supersonic flow. The basic expression for plane flow

In a way similar to that used for unsteady one-dimensional flow, we introduce the analogous expression for plane flow. We make use of the equation in the

characteristic direction by assuming that the curvature of the characteristics is small (see Howarth 1953, p. 75):

$$\frac{\partial v_\alpha}{\partial \alpha} - \frac{v_\alpha}{v_\beta}\frac{\partial v_\beta}{\partial \alpha} + \frac{v_\alpha}{\rho v_\beta^2}\frac{\partial p}{\partial \alpha} = 0. \tag{8.1}$$

Here, α and β are the characteristic and the orthogonal curvilinear co-ordinates, respectively, p is the pressure, and v_α, v_β are the velocity components in the α

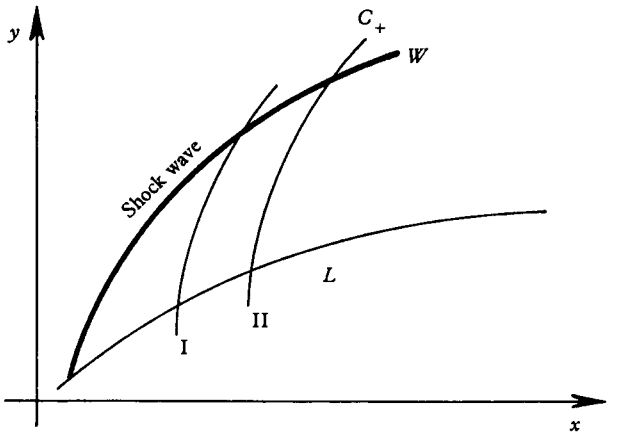

FIGURE 21. The boundary-value problem in plane steady supersonic flow.

and β directions, respectively. We take the α-co-ordinate along the C_+ characteristic. The compatibility equations for an oblique shock wave can be written in the form (see Stanjukovitch 1955)

$$V_W = V_1 \frac{\cos\gamma}{\cos(\gamma-\theta)}, \tag{8.2}$$

where γ, θ are defined in figure 22,

$$\frac{p_W}{p_1} = \frac{2k}{k+1} M_1^2 \sin^2\gamma - \frac{k-1}{k+1}, \tag{8.3}$$

$$\frac{2}{k-1} = M_1^2 \sin^2\gamma \left[\frac{k-1}{k+1}\frac{\tan(\gamma-\theta)}{\tan\gamma} - 1\right]. \tag{8.4}$$

From these equations we obtain

$$v_{\alpha W} = V_W \cos\mu_2 = V_1 \frac{\cos\gamma\cos\mu_2}{\cos(\gamma-\theta)} \equiv f(\gamma, V_1), \tag{8.5}$$

$$v_{\beta W} = V_W \sin\mu_2 \equiv \phi(\gamma, V_1), \tag{8.6}$$

$$p_W = \psi(\gamma, V_1), \tag{8.7}$$

where the Mach angle $\mu_2 = \sin^{-1} 1/M_2$. We assume that we can express all the parameters of the flow in terms of the velocity V_1 in front of the shock wave. The boundary-value problem can then be presented in a similar way as in § 2. We assume that we are given an arbitrary curve L which is not a characteristic (it can be the surface of a body, see figure 21), and that on this curve the boundary conditions $V = V_L(x)$, $p = p_L(x)$ are given.

As before in § 2, we integrate the expression (8.1) along a C_+ characteristic between the L-line and the shock wave. Expressing the values on the shock wave by equations (8.5), (8.6) and (8.7), we obtain

$$f(\gamma, V_1) - v_{\alpha_L} - \int_{v_{\beta L}}^{\phi(\gamma, V_1)} \frac{v_\alpha}{v_\beta} dv_\beta + \int_{p_L}^{\psi(\gamma, V_1)} \frac{v_\alpha}{\rho v_\beta^2} dp = 0.$$

Applying the above equation to two neighbouring characteristics $C_{+\mathrm{I}}$ and $C_{+\mathrm{II}}$ (see figure 21), and subtracting one of these relations from the other, we obtain in the limit as $C_{+\mathrm{I}} \to C_{+\mathrm{II}}$

$$\begin{aligned} &f'_\gamma(\gamma, V_1)\, d\gamma + f'_{V_1}(\gamma, V_1)\, dV_1 - dv_{\alpha_L} - \left[\frac{v_\alpha}{v_\beta}\right]_W [\phi'_\gamma(\gamma, V_1)\, d\gamma + \phi'_{V_1}(\gamma, V_1)\, dV_1] \\ &+ \left[\frac{v_\alpha}{v_\beta}\right]_L dv_{\beta_L} - \left[d\left(\frac{v_\alpha}{v_\beta}\right)\right]_m [\phi(\gamma, V_1) - v_{\beta_L}] + \left[\frac{v_\alpha}{\rho v_\beta^2}\right]_W [\psi'_\gamma(\gamma, V_1)\, d\gamma + \psi'_{V_1}(\gamma, V_1)\, dV_1] \\ &- \left[\frac{v_\alpha}{\rho v_\beta^2}\right]_L dp_L + \left[d\left(\frac{v_\alpha}{\rho v_\beta^2}\right)\right]_m [\psi(\gamma, V_1) - p_L] = 0. \end{aligned} \tag{8.8}$$

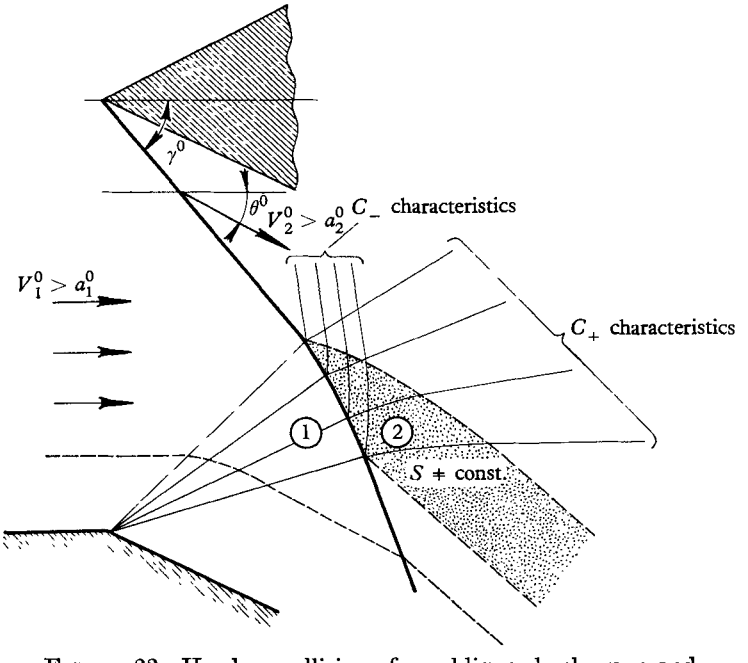

FIGURE 22. Head-on collision of an oblique shock wave and a Prandtl–Meyer expansion in steady plane flow.

Here values with the suffix m are the mean values in the interval of integration. In the linearized case, all the parameters can be written as $V = V_L + \epsilon_v$, etc., where $\epsilon_v \ll V_L$, etc. We see that the terms with mean values are small quantities of the second order. Neglecting these, we obtain

$$\begin{aligned} &f'_\gamma(\gamma, V_1)\, d\gamma + f'_{V_1}(\gamma, V_1)\, dV_1 - \left[\frac{v_\alpha}{v_\beta}\right]_W [\phi'_\gamma(\gamma, V_1)\, d\gamma - \phi'_{V_1}(\gamma, V_1)\, dV_1] \\ &+ \left[\frac{v_\alpha}{\rho v_\beta^2}\right]_W \psi'_\gamma(\gamma, V_1)\, d\gamma + \left[\frac{v_\alpha}{\rho v_\beta^2}\right]_W \psi'_{V_1}(\gamma, V_1)\, dV_1 = dv_\alpha - \left[\frac{v_\alpha}{v_\beta}\right]_L dv_{\beta_L} + \left[\frac{v_\alpha}{\rho v_\beta^2}\right]_L dp_L. \end{aligned} \tag{8.9}$$

We shall henceforth apply equation (8.9) as an approximation for cases in which linearization is not valid. This equation is analogous to equation (2.9) for unsteady flow.

We shall now make use of this expression to solve the problems of the interaction of a Prandtl–Meyer expansion and an oblique shock wave, and plane hypersonic flow around a body.

9. Head-on collision of an oblique shock wave and a Prandtl–Meyer expansion

In a similar way to that for the unsteady wave interaction discussed in § 6, we now apply the relation (8.9) to the head-on collision of a simple rarefaction wave (Prandtl–Meyer flow) and an oblique shock wave (figure 22).

In front of the shock wave, the following equations are satisfied by the Prandtl–Meyer flow

$$\frac{V_1^2}{2}+\frac{a_1^2}{k-1}=\frac{a_0^2}{k-1}, \tag{9.1}$$

$$\frac{p_1}{p_1^0}=\left(\frac{a_1}{a_1^0}\right)^{2k/(k-1)}, \tag{9.2}$$

$$\theta_1=\sqrt{\left(\frac{k+1}{k-1}\right)}\tan^{-1}\sqrt{\left\{\frac{k+1}{k-1}(M_1^2-1)\right\}}-\tan^{-1}\sqrt{(M_1^2-1)}. \tag{9.3}$$

With these relations, we obtain from equation (8.9) the following expressions:

$$\frac{d\gamma}{dV_1}=\frac{M^2\bar{a}^2\sin\mu_W\left(G-\dfrac{B_1}{B_2}\right)\dfrac{a_0^2}{a_1^2}-\dfrac{\cos\mu_W}{\bar{\rho}k}\left(kM_1P_1-P_2\dfrac{a_0^2}{a_1^2}+P_3\dfrac{B_1}{B_3}\dfrac{a_0^2}{a_1^2}\right)}{\dfrac{B_2}{B_3}\left[M^2\bar{a}^2\sin\mu_W-\dfrac{P_3}{\bar{\rho}k}\right]a_1}, \tag{9.4}$$

where

$$\left.\begin{aligned}
&\bar{a}=\frac{a_W}{a_1},\quad \bar{\rho}=\frac{\rho_W}{\rho_1},\quad M=\frac{V_W}{a_W},\\
&G=\frac{\partial\theta_1}{\partial M_1}=\frac{1}{1-\dfrac{k-1}{k+1}(M_1^2-1)}\frac{M_1}{\sqrt{(M_1^2-1)}}-\frac{1}{M_1\sqrt{(M_1^2-1)}},\\
&B_1=2M_1\sin^2\gamma\left[\frac{k+1}{k-1}\frac{\tan(\gamma-\theta)}{\tan\gamma}-1\right],\\
&B_2=M_1^2\left\{\sin 2\gamma\left[\frac{k+1}{k-1}\frac{\tan(\gamma-\theta)}{\tan\gamma}-1\right]+\frac{k+1}{k-1}\left[\frac{\sin\gamma\cos\gamma}{\cos^2(\gamma-\theta)}-\tan(\gamma-\theta)\right]\right\},\\
&B_3=-M_1^2\sin^2\gamma\frac{k+1}{k-1}\frac{1}{\tan\gamma\cos^2(\gamma-\theta)},\\
&P_1=\frac{\partial p_2}{\partial p_1}=\frac{2k}{k+1}M_1^2\sin^2\gamma-\frac{k-1}{k+1},\\
&P_2=\frac{1}{p_1}\frac{\partial p_2}{\partial M_1}=\frac{4k}{k+1}M_1\sin^2\gamma,\\
&P_3=\frac{1}{p_1}\frac{\partial p_2}{\partial\gamma}=\frac{4k}{k+1}M_1^2\sin\gamma\cos\gamma.
\end{aligned}\right\} \tag{9.5}$$

Using the compatibility equations for the shock wave (8.2), (8.3) and (8.4), and the equations (9.1) and (9.2), we can express all coefficients of equation (9.4) as functions of γ and V_1 alone. We then obtain a first-order ordinary differential equation for γ as a function of V_1. Numerical calculations on the basis of equation

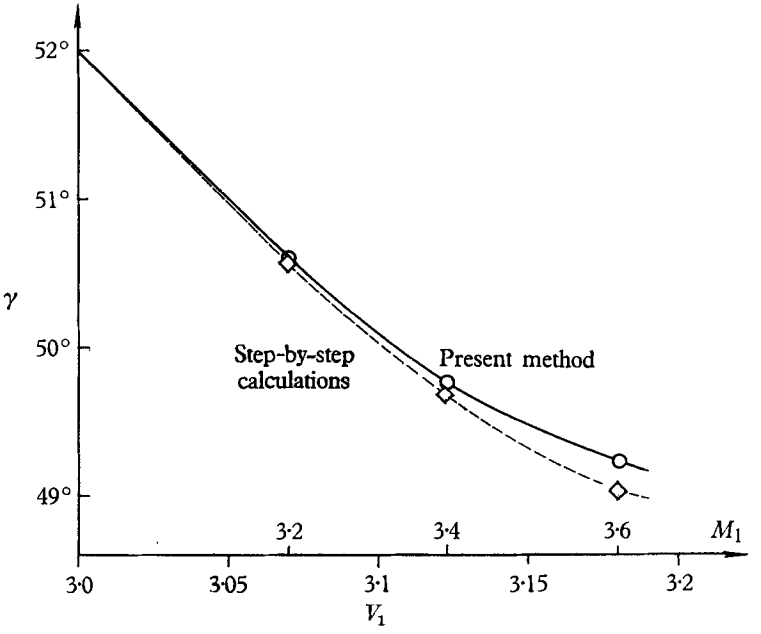

FIGURE 23. Comparison of the present method with the method of characteristics for the case of head-on collision of an oblique shock and a Prandtl–Meyer expansion.

(8.4) enable the computation of the shock-wave path without solving the partial differential equations governing the flow on the back of the shock wave. Equation (9.4) could be used to construct suitable tables.

A comparison of the results obtained with those of finite difference calculations is presented in figure 23 for $M_1^0 = 3$, $\gamma^0 = 52°$.

10. The shock wave in plane flow around a body

We consider the problem of the calculation of the shock-wave shape in plane supersonic flow around a body (see figure 24). We assume the shock wave to be attached (i.e. the nose angle of the body is smaller than the critical one). This problem corresponds to the merging shock and rarefaction wave in one-dimensional unsteady flow considered in § 6B.

Taking the body surface as a curve L and assuming that there is no reflected wave from the shock wave (a small reflexion is observed according to Egger's *et al.* (1955) paper), we can calculate all the parameters on the body surface from the Prandtl–Meyer flow relations. From (8.9) we obtain

$$\frac{d\gamma}{d\theta} = \frac{2V_L^2 \sin\mu_{2L}}{BV_W^2 \sin\mu_W + (p_1/\rho_W) P_3 \cos\mu_W}, \tag{10.1}$$

where B and P_3 are given by equations (9.5).

Expressing all the parameters in the denominator of equation (10.1) in terms of γ and in the numerator in terms of θ, we get the following equation

$$\int_{\gamma^0}^{\gamma} \Phi(\gamma)\, d\gamma = \int_{\theta_L^0}^{\theta_L} \psi(\theta_L)\, d\theta_L, \tag{10.2}$$

where $\Phi(\gamma)$, $\overline{U}(\theta_L)$ are functions given by the denominator and numerator in equation (10.1), respectively.

The equation gives the variation of the shock-wave angle γ as a function of the body shape given by θ_L, taken on the same characteristic.

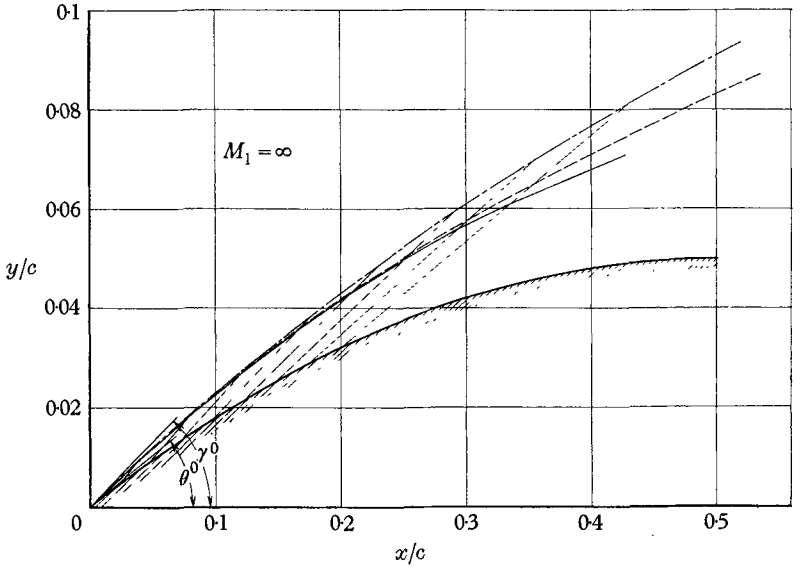

FIGURE 24. Supersonic plane flow around a body (the calculations by the method of characteristics and the shock expansion method are taken from Eggers *et al.* 1955). ——, Present method; – – – –, method of characteristics; ——·——, shock-expansion method.

This method differs from the shock-expansion method, where all the parameters are assumed to be constant along the C_+ characteristics (i.e. a simple wave). In the present solution θ varies along the characteristics. These solutions are the same only in the linearized case. However, the assumption that the C_+ characteristics are straight lines was made in the calculation of the shock-wave shape.

Figure 24 presents a comparison of the present theory, applied to a 10% thick biconvex airfoil at $M_1 = \infty$, with the results published in Egger's *et al.* paper obtained by the method of characteristics. (This comparison is not very accurate because the figure drawn in their paper is not precise.)

An interesting problem is the influence of the entropy change on the flow behind the shock wave. We obtain for oblique shock waves (in a similar way as in § 3) the following formula

$$\frac{1}{c_p}\frac{dS}{d\gamma} = 4\left\{\frac{M_1 \sin\gamma}{2kM_1^2\sin^2\gamma - k + 1} - \frac{1}{M_1 \sin\gamma[(k-1)M_1^2\sin^2\gamma + 2]}\right\} M_1 \cos\gamma. \tag{10.3}$$

For $M_1 = \infty$

$$\frac{1}{c_p}\frac{dS}{d\gamma} = \frac{2}{k}\cot\gamma. \tag{10.4}$$

We then get for a given curvature of the shock wave a weak entropy gradient behind the shock wave, and hence low vorticity for γ close to $\frac{1}{2}\pi$ (a detached shock wave).

For the given profile, it follows from the above method of shock-shape calculation that the higher the Mach number M_1, the smaller is the curvature of the shock wave. It therefore follows that the entropy change at higher Mach numbers is smaller because of the smaller curvature of the shock wave.

11. Discussion

The results obtained in the present paper seem to be very useful for many cases of non-uniform motion of shocks, detonation waves, and contact surfaces, but the present method enables us to find only the position of the unknown discontinuity line. In the case of small disturbances, when the linearized approximation can be applied, it is possible to find the complete flow field. In the general case, it is necessary for the determination of the flow field to solve the modified Cauchy problem for the basic partial differential equations with the boundary conditions given on the known discontinuity line.

The results obtained in this paper are very close to those obtained by step-by-step calculations based on the method of characteristic, because the neglected expressions containing mean values in equations (2.9) and (8.9) have small contributions. This is because the curvature of the α-characteristics is small in all the problems considered. The assumption of straight characteristics, which was made in some of the cases, gives results which differ little for both methods. This difference depends on the entropy change behind the shock wave.

In this paper the results obtained were compared with step-by-step calculations mainly for shock strengths $\overline{U} = 3, 4, 5$, where the influence of entropy changes is greatest. For weak and strong shocks the results are therefore better than for shocks of medium strength.

The author wishes to express his gratitude to Mr P. Kijkowski and Mr S. Pietrzyk for their help in carrying out the computations necessary for the examination of the present method; and also to the Fluid Mechanics Department of the Institute of Basic Problems of the Polish Academy of Sciences for financing this work.

REFERENCES

Billington, I. J. 1956 *J. Aero. Sci.* **23**, 997.

Chisnell, R. F. 1957 *J. Fluid Mech.* **2**, 286.

Courant, R. & Friedrichs, K. O. 1948 *Supersonic Flow and Shock Waves.* New York: Academic Press.

Eggers, A. J., Savin, R. C. & Syvertson, C. A. 1955. *J. Aero. Sci.* **22**, 231.

Friedrichs, K. O. 1948 *Commun. Pure Appl. Math.* **1**, 211.

Geiringer, H. 1948 *Advances in Applied Mechanics*, vol. I. New York: Academic Press.

GUNDERSEN, R. 1958 *J. Fluid Mech.* **4**, 501.

HERTZBERG, A. & KANTROWITZ, A. 1950 *J. Appl. Phys.* **21**, 874.

HOWARTH, L. 1953 *Modern Development in Fluid Dynamics: High-Speed Flow*, vol. I. Oxford University Press.

PAYNE, R. B. 1957 *J. Fluid Mech.* **2**, 185.

ROŚCISZEWSKI, J. 1958 Ph.D. Thesis. Published in *Archiwum Budowy Maszyn*, no. 1, 1959.

STANJUKOVITCH, K. P. 1955 *Non-Steady Motion of Continuous Media.* Moscow.

WHITHAM, G. B. 1958 *J. Fluid Mech.* **4**, 337.